Short Communication

Preparation of ZnO Porous Nanostructures and Its Application in Cathode Material for Lithium Sulfur Battery

Xinghua Liang[1,*], Qingqing Song[1,*], Yusi Liu[2], Hao Liu[1]

[1]Guangxi Key Laboratory of Automobile Components and Vehicle Technology, Guangxi University of Science and Technology, Guangxi, Liuzhou 545600, China; [2]Shanghai Jiao Tong University, Shanghai 200240, China
[*]E-mail: lxh304@aliyun.com; 18677270132@163.com

ZnO porous nanostructures were prepared by a two-step method which is composed of hydrothermal process and heating treatment. S/ZnO composite materials were prepared by heat treatment a mixture of sulfur and ZnO porous nanostructures at 155℃. The crystal structure and morphology of the prepared samples were showed by X-ray diffractometry (XRD) and scanning electron microscope (SEM). The electrochemical properties of S/ZnO composites were studied by means of cyclic voltammetry (CV), electrochemical impedance spectroscopy (EIS) and the charge and discharge test. The electrochemical study shows that the S/ZnO cathode presents an initial discharge capacity of 1414 mAh·g-1 and retains 662 mAh·g-1 with a Columbic efficiency 97% after 100 discharge/charge cycles at the current density of 335 mA·g-1 between 1.0 and 2.8V.

1. INTRODUCTION

The lithium/sulfur system, based on the chemical reaction process $16Li+S_8 \leftrightarrow 8Li_2S$, is one of the most potential secondary batteries for high-energy density and high-power density applications, due to its low cost, abundance, environmental friendliness, high theoretical capacity of 1675mAh·g^{-1} and gravimetric energy density of 2600Wh·kg^{-1} [1-5]. However, the practical development of the lithium/sulfur battery still suffers from several serious problems, such as insulating property of sulfur and its reduced products (Li_2S/Li_2S_2) [6,7] and the dissolution of polysulfides ($Li_2S_n, 4 \leq n \leq 8$) [8,9].

Different methods have been put forward to solve the above problems, among which preparation of nano scale materials is considered as an effective solution. Various nanosized and

nanostructured materials, such as zero dimension porous carbon [10], nanotubes/nanofibers [11], and core/yolk-shell structure [12,13], have been used to improve the conductive properties of sulfur cathode and inhibit the dissolution of polysulfides in organic electrolyte. Wang et al.[14] has reported a multiwalled carbon nanotubes-sulfur composites material prepared by chemical activation multiwalled carbon nanotubes and capillary effect of mixture. The composite material shows good cycle stability and rate capability due to the interstitial structure of the multiwalled carbon nanotubes. Besides, metal oxides for polysulfides retardation have attracted attention,such as $Mg_{0.6}Ni_{0.4}O$[15], Al_2O_3[16], and TiO_2[17]. Choi et al.[18] revealed that nano-sized Al_2O_3 particles can effectively inhibit the dissolution of the polysulfides in organic electrolyte and the sulfur/ Al_2O_3 composites show a high discharge capacity of 660 mAh·g^{-1}.

In this work, ZnO porous nanostructures are prepared by a facile hydrothermal method and subsequent calcinations at higher temperature. Compared with the pure sulfur electrode, the obtained S/ZnO composites show higher initial discharge capacity, excellent rate capability and good cycle life.

2. EXPERIMENTAL

2.1 Materials preparation

The ZnO porous nanostructures materials were synthetized by hydrothermal process: 0.825g $Zn(CH_3COO)_2·2H_2O$ and 3.75g glucose were poured into 30 ml deionized water under magnetic stirring for 10min. The mixed solution was transferred into 50 ml autoclave and heated at 180℃ for 20h. The black precipitate was washed with deionized water and ethanol and then maintained 10h at 80 ℃. Finally, the product was annealed at 600℃ for 2h with a heating rate of 2℃·min^{-1}.

The S/ZnO composite materials were synthesized by a melt-diffusion method. At first, 1:3 mass ratios of the ZnO materials and sublimed sulfur were mixed and milled in the ball milling tank for 1h.Subsequently, the composite was heated at 155℃ for 8h in a tubular furnace under Ar atmosphere.

2.2 Material characterization

The morphology of the prepared samples were showed by scanning electron microscopy (SEM, ZEISS) X-ray diffractometer (XRD, Bruker D8 Advance; Cu Kα radiation: λ=0.154184 nm) was applied to identify the crystalline characteristics of ZnO and the prepared S/ZnO composites.

2.3 Cell assembly and characterization

The electrodes were prepared by mixing 80wt% sulfur/ZnO materials, 10wt% conductive carbon black and 10wt% polyvinylidene fluoride (PVDF) in 1-methyl-2-pyrrolidinone (NMP) solvent

to form a homogeneous slurries. Then, the prepared slurries were spread onto Al foil (30μm in thickness) and were dried at 60℃ for 12h. The CR2016 coin type cells were assembled by sulfur/ZnO cathode, Celgard 2325 separator and Li anode in an argon-filled glove box. The electrolyte was 1mol·L^{-1} LiPF6 in a mixed solvent of 1,3-dioxolane (DOL) and 1,2-dimethoxyethane (DME) (1:1,v/v). Cyclic voltammetry and electrochemical impedance spectroscopy were obtained from the electrochemical workstation (CHI660E) at the scan rate of 0.2 mV·s^{-1} and the frequency range between 10^{-2}Hz and 10^{5}Hz with a perturbation amplitude of 5mV, respectively.

3. RESULTS AND DISCUSSION

3.1 Structural and morphology characterization

The X-ray diffraction(XRD) patterns of elemental sulfur, ZnO and S/ZnO composite are shown in Fig.1. It can be clearly observed that all the diffraction peaks of ZnO nanostructures are consistent with the hexagonal ZnO lattice (JCPDS No. 36-1451)[19,20]. Besides, no other diffraction peaks are founded, which indicates the products are a high purity hexagonal wurtzite ZnO phase. the XRD pattern of S/ZnO composite is similar to the ZnO and exhibits some low-intensity peaks of sulfur between 20° and 30°. It may indicate that some sulfur particles are absorbed on the ZnO materials.
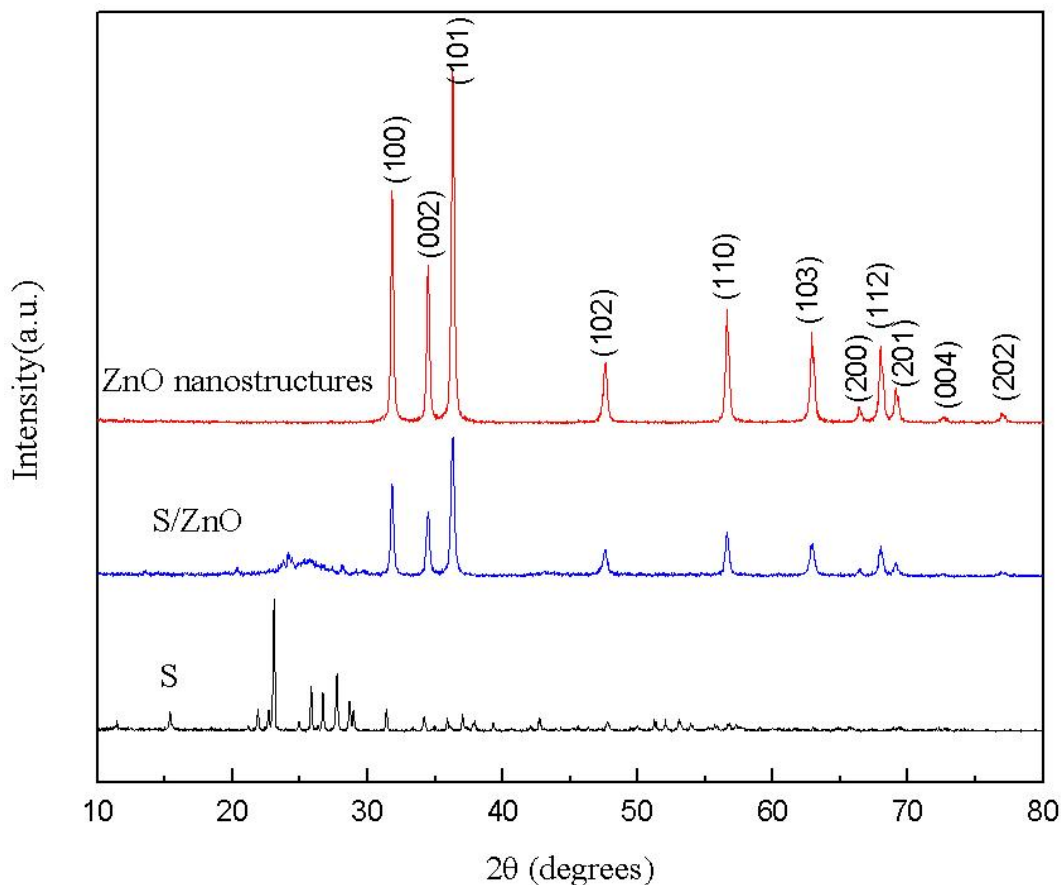

Figure 1. The XRD patterns of sulfur, ZnO and sulfur/ZnO composite.

SEM images of the ZnO porous nanostructures and S/ZnO composites are shown in Fig. 2. It is clearly seen from the low magnification image in Fig. 2a that the product synthesized by hydrothermal process and subsequent annealing consists of carpet-like structures. The close observation shows that these carpet-like structures are composed of a large number of nanoparticles in the size range of ~30-60nm as shown in Fig. 2b. Fig. 2c demonstrates that the size of S/ZnO is slightly larger than that of ZnO due to some sulfur absorbing onto the ZnO surface[21].
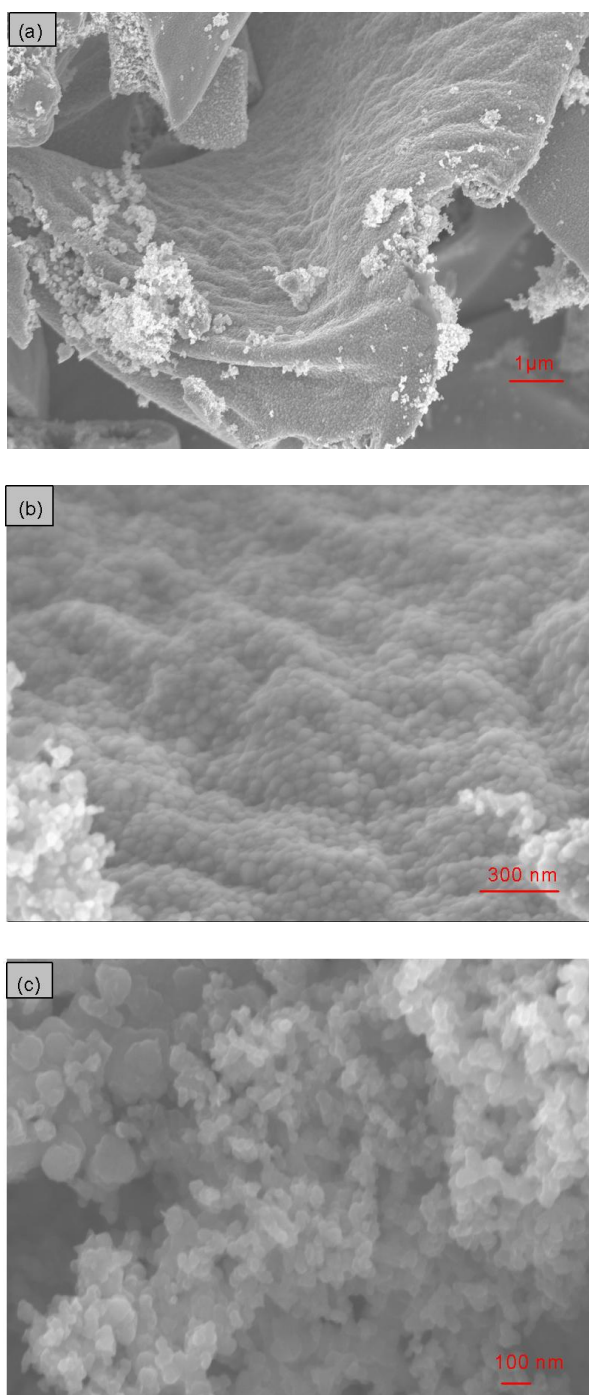
Figure 2. SEM images of (a) and (b) ZnO nanostructures, (c) S/ZnO composite.

3.2. Electrochemical performance

Fig. 3(a) shows the CV curve of the S/ZnO electrode in the voltage range between 1.0V and 2.8V with a scanning rate of 0.2 mV·s^{-1}. There are two voltage plateaus at about 1.95V and 2.2V in the discharge process and one voltage plateau at about 2.5-2.6V in the charge process. The first reduction peak at about 2.2V is corresponding to the transformation of Sulfur to high-order polysulfides, and the second reduction peak at 1.95V indicates the further reduction of lithium polysulfides to Li_2S_2/Li_2S[4,22]. The voltage platform at about 2.5-2.6V in the charging process refers to the oxidation of Li_2S to high-order polysulfides[23].

Discharge/charge curves of pure S and S/ZnO at the first and 100th cycles at 0.2C (1C=1675 mA·g^{-1}) are shown in Fig. 3(b). The discharge voltage curves of the S/ZnO composite cathode display two plateaus corresponding to the two step reduction reaction of lithium sulfur battery as illustrated in CV measurements (Fig. 3(a)). The initial discharge capacity of S/ZnO cathode is 1414 mAh·g^{-1} and drops to 662 mAh·g^{-1} after 100 discharge/charge cycles, which is clearly better than the initial discharge capacity of pure S.
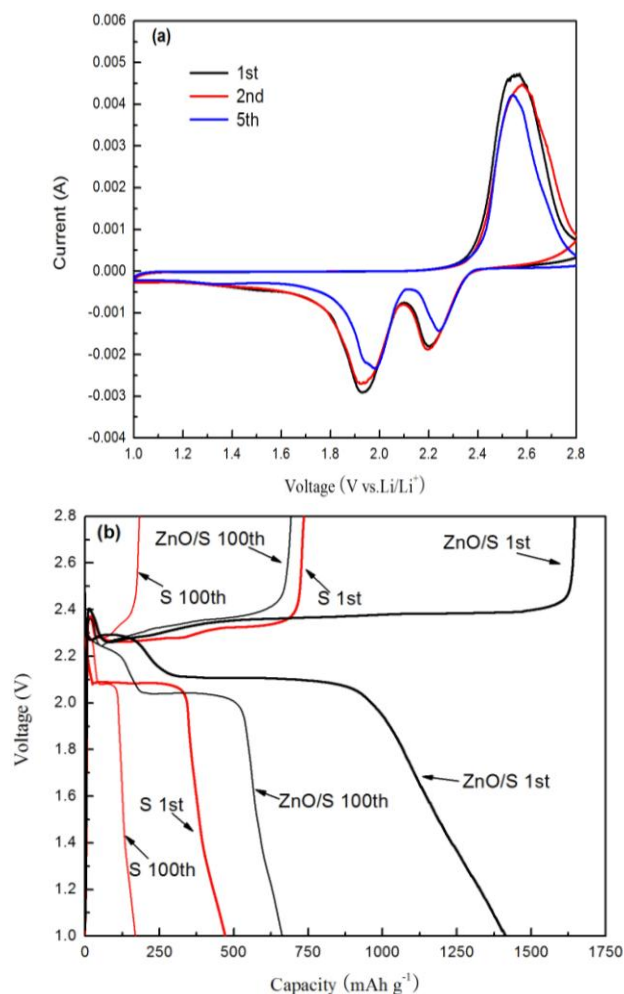

Figure 3. (a) CV curves of the S/ZnO composite at 0.2mV·s^{-1} . (b) Discharge and charge curves of pure S and S/ZnO at the first and 100th cycles.

Cycling discharge capacity and coulombic efficiency of pure S and S/ZnO at 0.2C between 2.8V and 1.0V are shown in Fig. 4(a). The S/ZnO composite shows the discharge capacities of 1414mAh·g^{-1} for the initial cycle and 662mAh·g^{-1} after 100 discharge/charge cycles, respectively. However, the discharge capacity of pure S is 470mAh·g^{-1} for the initial cycle and decrease to 169mAh·g^{-1} after 100 cycles. It is clear that the cycling stability and discharge capacity of the S/ZnO composite are higher than that of pure S. Besides, the average coulombic efficiency of S/ZnO cathode is 94.7%, which shows that self-discharge reaction of Li-S cell and the shuttle effect are not apparent[24].
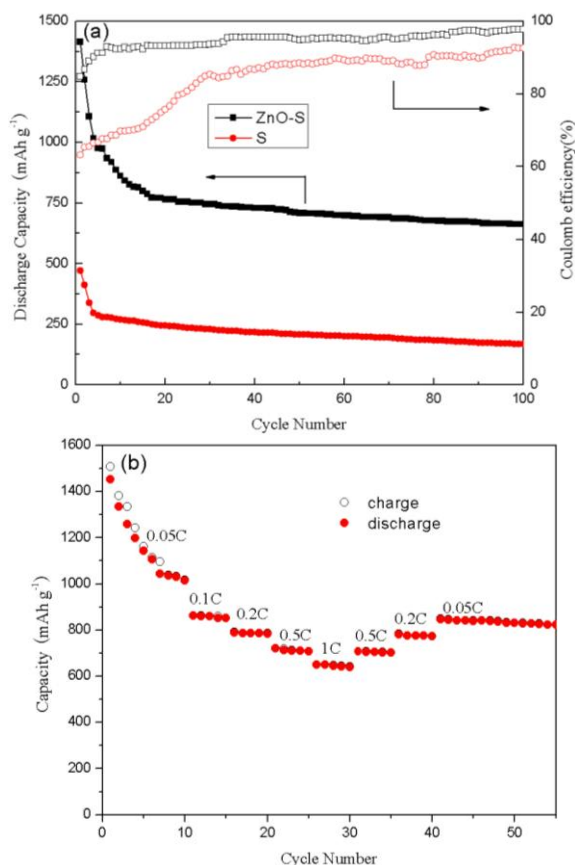

Figure 4. (a)Cycle performance and coulombic efficiency of pure S and the S/ZnO composite cathode. (b) Rate performance of the S/ZnO composite cathode.

Rate performance of S/ZnO at different current densities is shown in Fig. 4(b). During the first ten cycles, the discharge capacity of S/ZnO composite cathode reduced gradually from 1451mAh·g^{-1} to 1014mAh·g^{-1} at 0.05C rate. When the discharge/charge rate gradually enhanced from 0.1C to 1C, the S/In2O3 composite electrode showed the discharge capacities of 851mAh·g^{-1}, 784mAh·g^{-1}, 707mAh·g^{-1}, 639mAh·g^{-1}, respectively. And then the discharge/charge rate gradually returned to 0.5C, 0.2C and 0.05C, the discharge capacity of S/ZnO composite cathode is 703 mAh·g^{-1}, 773 mAh·g^{-1}, 822 mAh·g^{-1}, respectively. The test result suggests that the nanostructure of ZnO is benefit to improve the stability of the cathode material.

Fig. 5 shows electrochemical impedance spectra of the S/ZnO cathode at different cycle

numbers and the equivalent circuits. It can be seen that the Nyquist plots of the electrode are composed of a semicircle at the high-frequency region and an inclined line at the low-frequency region. The high-frequency intercept on the real axis corrsponds to the ohmic resistance (R1) including the electrolyte and cell components resistances[25]. The semicircle represents the interface charge-transfer resistance (R2), and the inclined line relates to Warburg impedance (Wo)[11,26,27]. It can be seen that the R1 value no obvious change during 100 cycles. It indicates that little lithium polysulfide dissolved in electrolyte during cycling. The value of R2 calculated from the semicircle decreases from 353.8Ω before 1st discharge to 32.42Ω after 50th charge, indicating the conductivity increase[28] and the improved reaction kinetics[29] of the S/ZnO cathode.
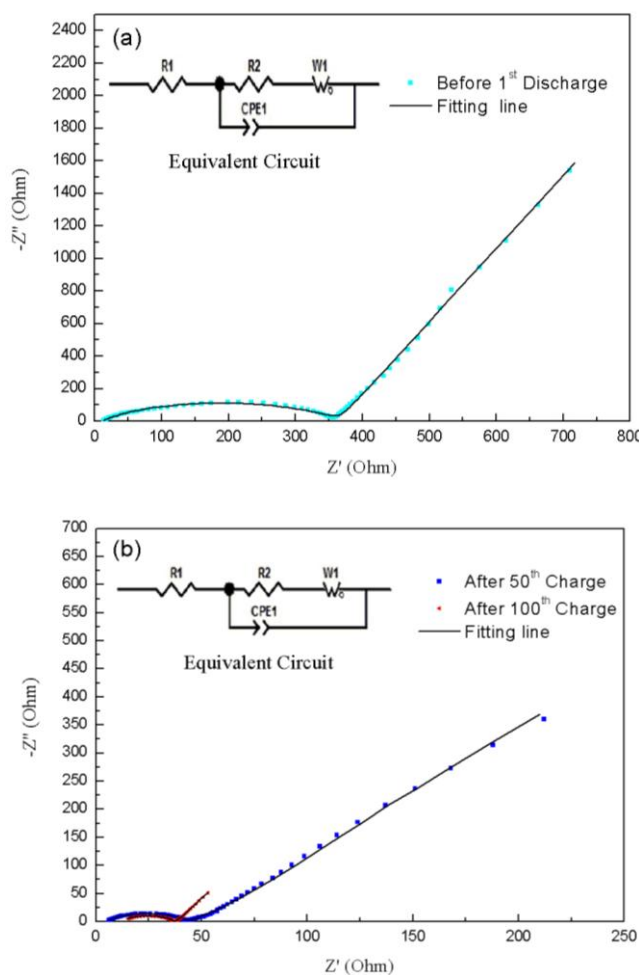

Figure 5. Nyquist plots and the equivalent circuit of the S/ZnO cathode (a) before cycling and (b) after 50th and 100th cycles.

4. CONCLUSION

Porous ZnO nanostructures have been successfully synthesized by hydrothermal method and heating treatment. S/ZnO composite materials were prepared by heat treatment a mixture of sulfur and ZnO porous nanostructures at 155℃ and then cell was assembled. The S/ZnO can deliver an initial

discharge capacity of 1414 mAh·g^{-1} and retains 662 mAh·g^{-1} with a Columbic efficiency 97% after 100 discharge/charge cycles at the current density of 335 mA·g^{-1}. however, the discharge capacity of pure S is 470mAh·g^{-1} for the initial cycle and decrease to 169mAh·g^{-1} after 100 cycles. It is clear that the cycling stability and discharge capacity of the S/ZnO composite are higher than that of pure S. These results indicate that the porous ZnO nanostructures is a promising host material for the sulfur cathode for lithium sulfur battery.

References

1. R. Noorden, *Nature* ,498 (2013) 416.
2. A. Manthiram, Y. Fu and Y. Su, *Acc. Chem. Res.*, 45 (2013) 1125.
3. J. Nelson, S. Misra, Y. Yang, A. Jackson, Y. Liu, H. Wang, H. Dai, J.C. Andrews, Y. Cui and M.F. Toney, *J. Am. Chem. Soc.*, 134 (2012) 6337.
4. Y.X. Wang, S.L. Chou, H.K. Liu and S.X. Dou, *J. Power Sources,* 244 (2013) 240.
5. L.L. Xie, Y.D. Xu, J.J. Zhang, X.Y. Cao, B. Wang, X.Y. Yan and L.B. Qu, *Int. J. Electrochem. Sci.*, 8 (2013) 1701.
6. S. Evers and L. Nazar, *Acc. Chem. Res.*, 46 (2013) 1135.
7. Y.S. Su and A. Manthiram, *Electrochim. Acta* , 77 (2012) 272.
8. G. He, X. Ji and L. Nazar, *Energy Environ. Sci.*, 4 (2011) 2878.
9. Z.S. Wen, D. Lu, S. Li, J.C. Sun and S.J. Ji, *Int. J. Electrochem. Sci.*, 9 (2014) 1.
10. N.D. Petkovich and A. Stein, *Chem. Soc. Rev.*, 42 (2013) 3721.
11. M. Rao, X. Song, H. Liao and E.J. Cairns, *Electrochim. Acta*, 65 (2012) 228.
12. L. Yin, J. Wang, J. Yang and Y. Nuli, *J. Mater. Chem.*, 21 (2011) 6807.
13. W. Zhou, Y. Yu, H. Chen, F.J. DiSalvo and H.D. Abruna, *J. Am. Chem. Soc.*, 135(2013) 16736.
14. X. Z. Ma, B. Jin, P. M. Xin and H. H. Wang, *Applied Surface Science.*, 307 (2014) 346.
15. Y. Zhang, Z. Bakenov, Y. Zhao, A. Konarov, L. Doan, K. Sun and P. Chen, *Powder Technol.*, 235 (2013) 248.
16. K. Dong, S. Wang, H. Zhang and J. Wu, *Mater. Res. Bull.*, 48 (2013) 2079.
17. S. Evers, T. Yim and L. Nazar, *J. Phys. Chem. C*, 116 (2012) 19653.
18. Y.J. Choi, B.S.Jung, D.J.Lee, J.H.Jeong, K.W.Kim, H.J.Ahn, K.K.Cho and H.B.Gu, *Phys. Scr.*, T129 (2007) 62.
19. A. Kajbafvala, S. Zanganeh, E. Kajbafvala, H.R. Zargar, M.R. Bayati and S.K. Sadrnezhaad, *J AlloysCompd*, 497 (2010) 325.
20. B.J. Li, L.J. Huang, M. Zhou and N.F. Ren, *MaterLett*, 110 (2013) 160.
21. E. Dujardin, T.M. Ebbesen, H. Hiura and K. Tanigaki, *Science* , 265 (1994) 1850.
22. Y.J. Li, H. Zhan, S.Q. Liu, K.L. Huang and Y.H. Zhou, *J. Power Sources*, 195 (2010) 2945.
23. J.C. Guo, Z.C. Yang, Y.C. Yu, H.D. Abrun and L.A. Archer, *J. Am. Chem. Soc.*, 135 (2013) 763.
24. G. Zheng, Y. Yang, J.J. Cha, S.S. Hong and Y. Cui, *Nano Lett.*, 11 (2011) 4462.
25. N.A. Canas, K. Hirose, B. Pascucci, N. Wagner, K.A. Friedrich and R. Hiesgen, *Electrochim. Acta*, 97 (2013) 42.
26. V.S. Kolosnitsyn, E.V. Kuz'mina, E.V. Karaseva and S.E. Mochalov, *Russ. J. Electrochem.*, 47 (2011) 793.

27. J. Zheng, M. Gu, H. Chen, P. Meduri, M.H. Engelhard, J. Zhang, J. Liu and J. Xiao, *J.Mater. Chem.*, A 1 (2013) 8464.
28. H. Wu, G.H. Yu, L.J. Pan, N. Liu, M.T. McDowell, Z.N. Bao and Y. Cui, *Nat.Commun.*, 4 (2013) 1943.
29. J.C. Guo, X.L. Chen and C.S. Wang, *J. Mater. Chem.*, 20 (2010) 5035.